

On the short-range behavior of neutrino forces: from $1/r^5$ to $1/r^4$, $1/r^2$, and $1/r$

Xun-jie Xu^{a,b} and Bingrong Yu^{a,b}

^a*Institute of High Energy Physics, Chinese Academy of Sciences, Beijing 100049, China*

^b*School of Physical Sciences, University of Chinese Academy of Sciences, Beijing 100049, China*

E-mail: xuxj@ihep.ac.cn, yubr@ihep.ac.cn

ABSTRACT: The exchange of a pair of neutrinos between two objects, separated by a distance r , leads to a long-range effective potential proportional to $1/r^5$, assuming massless neutrinos and four-fermion contact interactions. In this paper, we investigate how this known form of neutrino-mediated potentials might be altered if the distance r is sufficiently short, corresponding to a sufficiently large momentum transfer which could invalidate the contact interactions. We consider two possible scenarios to open up the contact interactions by introducing a t -channel or an s -channel mediator. We derive a general formula that is valid to describe the potential in all regimes as long as the external particles remain non-relativistic. In both scenarios, the potential decreases as $1/r^5$ in the long-range limit as expected. In the short-range limit, the t -channel potential exhibits the Coulomb-like behavior (i.e. proportional to $1/r$), while the s -channel potential exhibits $1/r^4$ and $1/r^2$ behaviors.

Contents

1	Introduction	1
2	Neutrino forces from contact interactions	3
3	Short-range behavior of neutrino forces	4
3.1	The t -channel behavior	4
3.2	The s -channel behavior	8
4	Summary	10
A	Renormalization of the ϕ propagator	10
B	Branch cuts and singularities of the amplitude	12

1 Introduction

The long-range forces arising from the exchange of a pair of neutrinos between two objects (the so-called neutrino forces) have been an old and interesting topic dating back to early considerations in the 1930s [1], subsequently followed by quantitative calculations in the 1960s [2]. In the framework of the Standard Model (SM), the (spin-independent part of the) effective potential between two electrons, induced by massless neutrino exchange, is formulated as [2–4]:

$$V_{ee}(r) = \left(2 \sin^2 \theta_W + \frac{1}{2}\right)^2 \frac{G_F^2}{4\pi^3} \frac{1}{r^5}, \quad (1.1)$$

where G_F is the Fermi constant, θ_W is the Weinberg angle, and r is the distance between two electrons. Early derivations [2, 3, 5] by Feinberg and Sucher employed the dispersion technique¹ and the result was verified by other authors via different approaches such as the Fourier transform [4] and the Hamiltonian formalism [7].

As has been well established by neutrino oscillation experiments, neutrinos have nonzero masses—see e.g. [8] for a recent review. The effect of neutrino masses on the long-range forces becomes non-negligible when the distance r exceeds $1/m_\nu$, where m_ν is the mass of the neutrino mediating the force. Including the mass effect, neutrino forces can be expressed in terms of the modified Bessel function [9], which in the long-range limit ($r \gg 1/m_\nu$) decreases exponentially as $\exp(-2m_\nu r)$. It is noteworthy that the effective potentials mediated by Dirac and Majorana neutrinos are different when neutrino masses can not be neglected [9], thus neutrino forces in principle could be used to determine the nature of neutrinos [10, 11]. In addition to the mass effect, further generalizations including the flavor mixing have been addressed in Refs. [7, 12].

Going beyond the standard Fermi interactions, one might consider neutrino forces between other particles such as dark matter (DM) [13], neutrino forces modified by neutrino magnetic moments [12],

¹See also Ref. [6] for a more pedagogical introduction.

or, instead of neutrinos, other light particles mediating similar long-range forces [14–21]. In Ref. [13], it has been shown that neutrino forces on DM could be sufficiently strong to impact small-scale structure formation in the early universe². Refs. [14, 17] studied systematically long-range forces arising from the exchange of two light particles of spin 0, 1/2, or 1. Ref. [14] showed that such forces could be used to search for DM in molecular spectroscopy and neutron scattering. It is interesting to note, as a conclusion of Ref. [17], that these potentials are necessarily attractive if the contact interactions are of the scalar form, despite whether the light particles are fermions or bosons.

In the aforementioned works, only contact interactions are considered, which for massless neutrinos necessarily lead to the $1/r^5$ form. Since such forces have been used to compute non-relativistic scattering cross sections of DM or nucleons where the momentum transfer might be considerably large (see e.g. [13, 14]), we take one step forward by asking to what extent the $1/r^5$ form remains valid at much smaller distances.

The $1/r^5$ form arises from the contact interaction, which can be seen by counting dimensions in Eq. (1.1). In the SM, as long as the external fermions are non-relativistic (otherwise the potential could not be well defined), the momentum transfer should be much smaller than the masses of W and Z bosons, which justifies the use of the contact interaction. As a consequence, when r decreases, the $1/r^5$ form remains valid until r approaches the inverse of the external fermion mass, in which case the non-relativistic approximation becomes invalid.

For non-SM interactions or particles (e.g. DM), however, the contact interaction might be invalid before the non-relativistic approximation fails. In this case, one needs to open the contact vertex between neutrinos and external fermions and recalculate the neutrino potential in a full renormalized theory. As we will show, if the contact vertex opens with a t -channel mediator ϕ , in the short-range limit where the mass of ϕ is negligible compared with the momentum transfer, one may expect that the potential reduces to a Coulomb-like form varying as $1/r$. Therefore, it is tempting to formulate a unified framework that describes the variation of the potential from $1/r^5$ (when $r \gg 1/m_\phi$) to $1/r$ (when $r \ll 1/m_\phi$), which will be presented in this work.

At the end of this introduction, we would like to briefly comment on the detection of neutrino forces. The SM neutrino force is extremely weak. From Eq. (1.1), one can estimate that only within the range of 10^{-8} cm can it overcomes the gravity. Nevertheless, new physics might enhance it to experimentally accessible level. Recently it has been proposed that in atomic systems, the existing constraints on neutrino forces from experiments that search for new macroscopic forces will be significantly improved on and the future spectroscopy experiments will be hopeful to probe such forces [32, 33].

The remaining part of this paper is organized as follows. In Sec. 2, we briefly revisit Feinberg and Sucher’s formalism to calculate the long-range neutrino potential from contact interactions. In Sec. 3, we embed the contact vertex into a full renormalized theory and investigate the short-range behavior of the neutrino forces. We consider two possible scenarios to open up the contact vertex by introducing a t -channel (Sec. 3.1) and an s -channel (Sec. 3.2) mediator. In both scenarios, we derive a general formula that is valid to describe the potential in all regimes as long as the external particles stay non-relativistic. We also show that the general formula will reduce to Feinberg and Sucher’s $1/r^5$ result in the long-range limit. Our main results and conclusions are summarized in Sec. 4. Finally, technical details about on-shell renormalization and calculation of the Fourier integrals using the discontinuity of the amplitude are given in two appendices.

²Cosmological effects of neutrino forces have been considered in early studies [22–24]. It is also worth mentioning that the many-body effect of neutrino forces in neutron stars once triggered a debate on the lower bound of m_ν [25–31].

2 Neutrino forces from contact interactions

In this section, we briefly review Feinberg and Sucher's formalism [2, 3, 5] to calculate the neutrino potential from a contact interaction. For simplicity, we assume a scalar-type interaction between neutrinos and the external fermions χ with mass m_χ

$$\mathcal{L}_{\text{int}} \supset G_S \bar{\chi} \chi \bar{\nu} \nu, \quad (2.1)$$

where G_S is a dimensional coupling constant. Here for simplicity we consider only one generation of neutrino and the interaction is non-chiral. Generalizations to chiral interactions or interactions with other Lorentz structures are straightforward. In addition, since we mainly focus on the short-range behavior of the potential, it is safe to neglect the mass of neutrino.

According to the Born approximation, the effective potential between two χ particles (or a pair of χ and $\bar{\chi}$ particles)³ is related to the non-relativistic elastic scattering amplitude $\chi\chi \rightarrow \chi\chi$ (or $\chi\bar{\chi} \rightarrow \chi\bar{\chi}$) by the Fourier transform

$$V(\vec{r}) = - \int \frac{d^3 \vec{q}}{(2\pi)^3} e^{i\vec{q} \cdot \vec{r}} \mathcal{A}_{\text{NR}}(\vec{q}), \quad (2.2)$$

where \vec{q} is the momentum transfer and $\mathcal{A}_{\text{NR}} \equiv \mathcal{M}_{\text{NR}} / (4m_\chi^2)$ is the (normalized) scattering amplitude in the non-relativistic limit, with the factor $1 / (4m_\chi^2)$ coming from normalization. For spin-independent scattering, \mathcal{A}_{NR} is only a function of $\rho \equiv |\vec{q}|$. Thus one can integrate out the angular part first to obtain a central potential

$$V(r) = \frac{i}{4\pi^2 r} \int_0^\infty d\rho \rho \mathcal{A}_{\text{NR}}(\rho^2) (e^{i\rho r} - e^{-i\rho r}) = \frac{i}{4\pi^2 r} \int_{-\infty}^\infty d\rho \rho \mathcal{A}_{\text{NR}}(\rho^2) e^{i\rho r}, \quad (2.3)$$

with $r \equiv |\vec{r}|$.

The scattering amplitude can be derived by calculating the left loop diagram in Fig. 1:

$$i\mathcal{A}(q^2) = -(iG_S)^2 \int \frac{d^4 k}{(2\pi)^4} \text{Tr} \left(\frac{i}{\not{k}} \frac{i}{\not{k} + \not{q}} \right) = \frac{iG_S^2}{8\pi^2} q^2 \left[2 + \Delta_E + \ln \left(\frac{\mu^2}{-q^2} \right) \right], \quad (2.4)$$

where q is the transferred four-momentum, μ is the renormalization scale and $\Delta_E \equiv 1/\epsilon - \gamma_E + \ln(4\pi)$ with $\epsilon \rightarrow 0_+$ and $\gamma_E \approx 0.577$ being the Euler–Mascheroni constant. Note that the normalized factor $1/(4m_\chi^2)$ has been cancelled by the non-relativistic wave functions of external fermions. In the non-relativistic limit, $q^2 \approx -\rho^2 < 0$, thus

$$\mathcal{A}_{\text{NR}}(\rho^2) = -\frac{G_S^2}{8\pi^2} \rho^2 \left[2 + \Delta_E - \ln \left(\frac{\rho^2}{\mu^2} \right) \right]. \quad (2.5)$$

Substituting Eq. (2.5) into Eq. (2.3), we have

$$V(r) = -\frac{iG_S^2}{32\pi^4 r} \int_{-\infty}^\infty d\rho \rho^3 \left[2 + \Delta_E - \ln \left(\frac{\rho^2}{\mu^2} \right) \right] e^{i\rho r} = -\frac{3}{8\pi^3} \frac{G_S^2}{r^5}. \quad (2.6)$$

³For scalar interactions, the resulting potentials are independent of whether they are χ or $\bar{\chi}$ particles. And the potentials are always attractive. Vector interactions, by contrast, lead to repulsive potentials between two χ particles of the same charge. This is similar to that tree-level scalar or vector mediators cause attractive or repulsive forces, see e.g. [34].

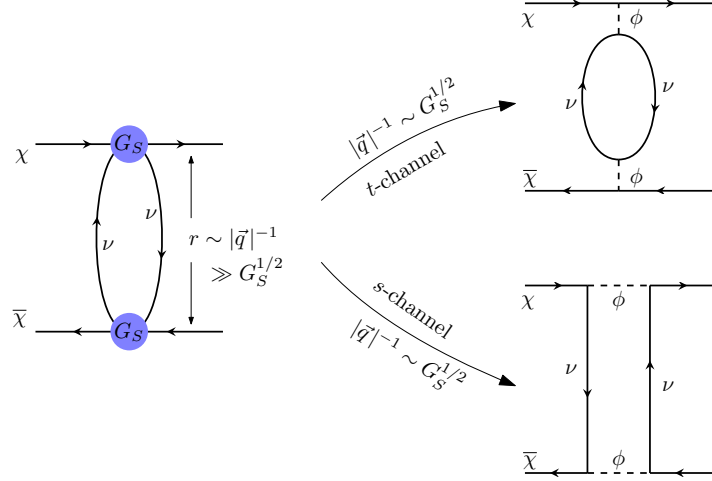


Figure 1. Neutrino forces from neutrino-pair exchange with a contact interaction (left diagram) and possible modifications (right diagrams) when the contact interaction is invalid due to $r \sim G_S^{1/2}$.

The Fourier integral can be computed by closing the contour on the complex plane of ρ —see Appendix B for more details.

It is interesting to note that, for contact interactions, the integrand in Eq. (2.6) does not contribute to the final result except for the logarithmic term, which has a branch cut on the imaginary axis in the complex plane. In particular, the UV divergent term does not appear in the effective potential, thus one only needs to extract the discontinuity at the branch cut (or equivalently, the imaginary part) of the amplitude and perform the integration along the imaginary axis.

3 Short-range behavior of neutrino forces

The neutrino-mediated potential derived from a contact interaction exhibits the $1/r^5$ behavior when r is large. As r decreases, the moment transfer $|\vec{q}| \sim r^{-1}$ between the two external fermions increases and can eventually exceed the energy scale of $G_S^{-1/2}$, above which the contact interaction is invalid. Therefore, when r is close to $G_S^{1/2}$ and the interaction becomes non-contact, we expect that the $1/r^5$ form should be altered.

To investigate the short-range behavior of neutrino forces, we consider two possible scenarios that the contact vertex may open up by introducing a t -channel (the upper right diagram in Fig. 1) or an s -channel (the lower right diagram) mediator.

3.1 The t -channel behavior

Let us first consider that the effective vertex is generated by a t -channel mediator. The Lagrangian reads:

$$\mathcal{L}_{\text{int}} \supset y_\nu \bar{\nu} \nu \phi + y_\chi \bar{\chi} \chi \phi , \quad (3.1)$$

where ϕ is a real scalar of mass m_ϕ , y_ν and y_χ denote the Yukawa couplings of ϕ to ν and χ , respectively.

In the long-range limit, ϕ can be integrated out and we obtain an effective four-fermion interaction, which reproduces Feinberg and Sucher's result: $V(r) \sim G_S^2/r^5$ with $G_S = y_\nu y_\chi / m_\phi^2$. This corresponds

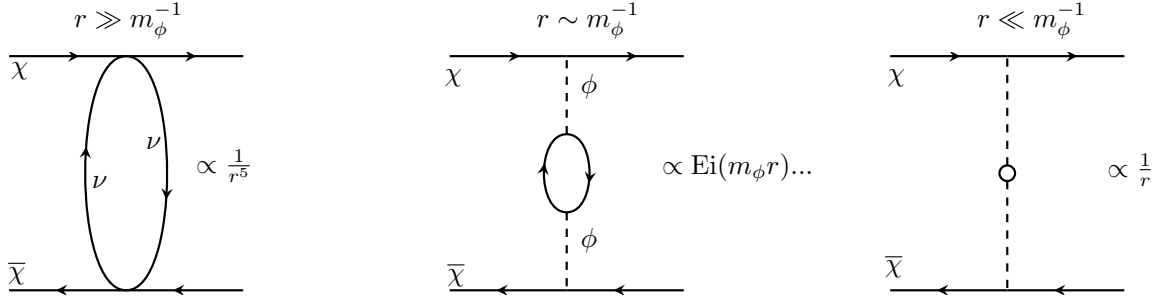


Figure 2. A diagrammatic explanation of the t -channel neutrino potential varying from the $1/r^5$ to the $1/r$ forms. In the long-range limit ($r \gg m_\phi^{-1}$), the potential decreases as $1/r^5$. At smaller distances ($r \sim m_\phi^{-1}$), the contact interaction vertices open up as two ϕ propagators. The resulting potential can be formulated in terms of the exponential integral function, $\text{Ei}(m_\phi r)$ —see Eqs. (3.4)-(3.5). Further reducing r to the short-range limit ($r \ll m_\phi^{-1}$), the neutrino loop becomes subdominant and the potential reduces to the Yukawa/Coulomb-like form, $1/r$.

to the first diagram in Fig. 2. Now consider that r decreases to small values so that $|\vec{q}|$ is comparable to m_ϕ . In this case, the contact interaction vertices are replaced by two ϕ propagators, corresponding to the second diagram. And the potential exhibits complicated r dependence involving the exponential integral function, $\text{Ei}(m_\phi r)$. Further reducing r , we expect that the ϕ propagators will play a more important role than the neutrino loop—illustrated by the last diagram. Eventually, with sufficiently small r , the effective potential is expected to be Yukawa- or Coulomb-like, $V \sim 1/r$.

Below we will show, via explicit calculations, that the potential indeed varies in this way.

First, we need to compute the non-relativistic scattering amplitude. The neutrino loop in this case is also UV divergent, similar to the previous calculation in Sec. 2. However, unlike the contact interaction case where the divergent and constant terms can be simply ignored, the UV divergence in this case requires a more careful treatment because, in addition to the branch cut from the logarithmic term, the scalar mediator contributes another type of singularities at $q^2 = m^2$. As a consequence, constant terms arising from the loop also contributes. Therefore, we need to identify the physical part of the constant terms, which can be obtained by embedding the one-particle-irreducible (1PI) diagram into the physical propagator of ϕ and perform on-shell renormalization. After the on-shell renormalization (see Appendix A for the details), we obtain the following scattering amplitude:

$$i\mathcal{A}(q^2) = \frac{iy_\chi^2 y_\nu^2}{8\pi^2 (q^2 - m_\phi^2)^2} \left[(q^2 - m_\phi^2) - q^2 \ln \left(\frac{-q^2}{m_\phi^2} \right) \right]. \quad (3.2)$$

In the non-relativistic limit, $q^2 \approx -\rho^2 < 0$ with $\rho \equiv |\vec{q}|$, we have

$$\mathcal{A}_{\text{NR}}(\rho^2) = \frac{y_\chi^2 y_\nu^2}{8\pi^2 (\rho^2 + m_\phi^2)^2} \left[-(\rho^2 + m_\phi^2) + \rho^2 \ln \left(\frac{\rho^2}{m_\phi^2} \right) \right], \quad (3.3)$$

which, after substituting into the Fourier transform (2.3), gives rise to the effective potential below

(for the detailed calculation, see Appendix B):

$$\begin{aligned} V_{\text{loop}}(r) &= \frac{iy_\chi^2 y_\nu^2}{32\pi^4 r} \int_{-\infty}^{\infty} d\rho \frac{\rho}{\left(\rho^2 + m_\phi^2\right)^2} \left[-(\rho^2 + m_\phi^2) + \rho^2 \ln\left(\frac{\rho^2}{m_\phi^2}\right) \right] e^{i\rho r} \\ &= \frac{m_\phi y_\chi^2 y_\nu^2}{64\pi^3} \mathcal{V}(m_\phi r), \end{aligned} \quad (3.4)$$

where

$$\mathcal{V}(x) \equiv \frac{2 + e^x (2 + x) \text{Ei}(-x) + e^{-x} (2 - x) \text{Ei}(x)}{x}, \quad (3.5)$$

and $\text{Ei}(x) \equiv -\int_{-x}^{\infty} dt \frac{e^{-t}}{t}$ is the exponential integral function.

The large and small x limits of $\text{Ei}(x)$ are given as follows:

- for $0 < x \ll 1$, $\text{Ei}(x) = (\gamma_E + \ln x) + x + \mathcal{O}(x^2)$, $\text{Ei}(-x) = (\gamma_E + \ln x) - x + \mathcal{O}(x^2)$;
- for $x \gg 1$, $\text{Ei}(x) = e^x \left[\frac{1}{x} + \mathcal{O}\left(\frac{1}{x^2}\right) \right]$, $\text{Ei}(-x) = e^{-x} \left[-\frac{1}{x} + \mathcal{O}\left(\frac{1}{x^2}\right) \right]$.

With the above limit, it is straightforward to obtain the asymptotic behaviors of $\mathcal{V}(x)$:

$$\mathcal{V}(x) = \begin{cases} \frac{2}{x} (1 + 2\gamma_E + 2\ln x) + \mathcal{O}(x) & (x \ll 1) \\ -\frac{24}{x^5} + \mathcal{O}\left(\frac{1}{x^7}\right) & (x \gg 1) \end{cases}. \quad (3.6)$$

Therefore, in the long-range limit, we have recovered Feinberg and Sucher's $1/r^5$ potential

$$V_{\text{loop}}(r) = -\frac{3y_\chi^2 y_\nu^2}{8\pi^3 m_\phi^4 r^5}, \quad r \gg m_\phi^{-1}, \quad (3.7)$$

which exactly matches the result of contact interaction in Eq. (2.6) with $G_S = y_\nu y_\chi / m_\phi^2$.

In the small-distance limit, the potential evolves with $\ln(r)/r$:

$$V_{\text{loop}}(r) = -\frac{y_\chi^2 y_\nu^2}{32\pi^3 r} \left[2 \ln\left(\frac{1}{m_\phi r}\right) - 1 - 2\gamma_E \right], \quad m_\chi^{-1} \ll r \ll m_\phi^{-1}. \quad (3.8)$$

One may observe that the potential in the small-distance limit becomes divergence if m_ϕ vanishes. This IR divergence can be removed when the neutrino mass effect is included.

Note that in the presence of the above Yukawa interactions, ϕ can directly mediate a Yukawa potential between two χ particles:

$$V_{\text{tree}}(r) = -\frac{y_\chi^2}{4\pi r} e^{-m_\phi r}. \quad (3.9)$$

At $r \gg 1/m_\phi$, the tree-level force is exponentially suppressed and the loop-level long-range neutrino force dominates. At small distances, both contribute while the neutrino force is, compared to Eq. (3.9), weaker by a factor of $y_\nu^2/(16\pi^2)$, which is the typical magnitude of loop suppression. Therefore, our calculations of the neutrino force induced by the neutrino loop can be alternatively viewed as a loop correction to the tree-level Yukawa force.

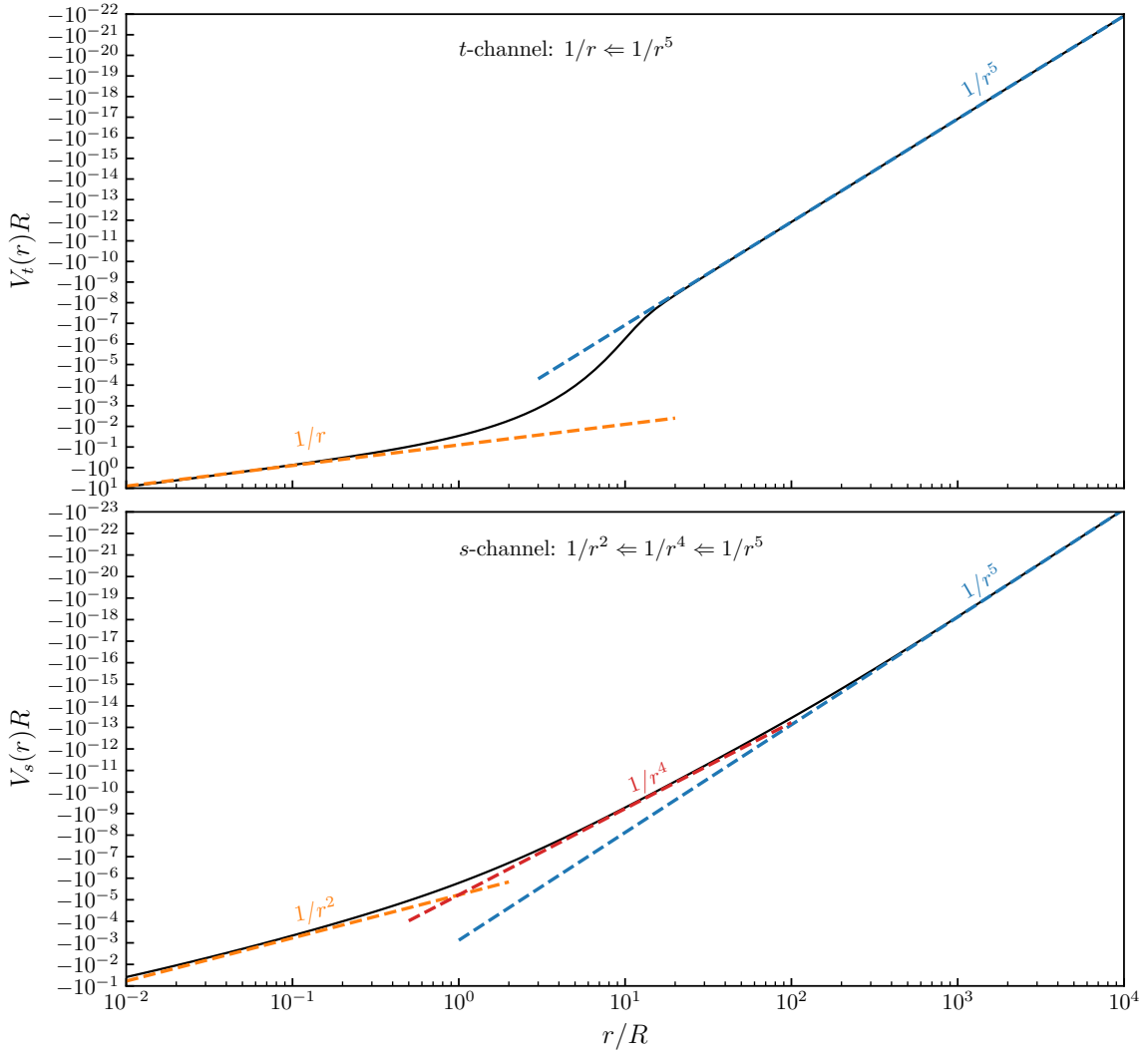


Figure 3. The evolution of the t -channel (upper panel) and s -channel (lower panel) effective potentials. In the long-range limit, both of the potentials decrease as $1/r^5$, while in the short-range limit, they exhibit $1/r$, $1/r^2$, or $1/r^4$ behaviors, depending on the UV completion of the contact interactions and relevant mass scales—see the text for further details and discussions. The length unit R is determined by m_ϕ and/or m_χ according to Eqs. (3.13) and (3.20).

In the spirit of a complete description of the potential, let us include the neutrino loop into the propagator of ϕ :

$$\frac{i}{q^2 - m_\phi^2} \rightarrow \frac{i}{q^2 - m_\phi^2 + \Sigma(q^2)}, \quad (3.10)$$

where $\Sigma(q^2)$ is the 1PI contribution. Computing the Fourier transform of the above loop-corrected propagator, one would obtain an effective potential that contains both contributions from the tree-level Yukawa force and the loop-level neutrino force. They correspond to the leading order and next-to-

leading order of the expansion in $\Sigma(q^2)$:

$$\frac{i}{q^2 - m_\phi^2 + \Sigma(q^2)} \approx \frac{i}{q^2 - m_\phi^2} - \frac{i}{(q^2 - m_\phi^2)^2} \Sigma(q^2) + \dots \quad (3.11)$$

Since our calculations are carried out only at the one-loop level, it is consistent to take only the first two terms in the expansion and take $\Sigma(q^2) \approx \Sigma_2(q^2)$, where $\Sigma_2(q^2)$ is the self-energy of ϕ to the order of $\mathcal{O}(y_\nu^2)$. This implies that we can obtain the full potential by simply adding Eq. (3.9) to Eq. (3.4):

$$V_t(r) = V_{\text{tree}}(r) + V_{\text{loop}}(r) = \frac{m_\phi y_\chi^2}{4\pi} \left[-\frac{e^{-m_\phi r}}{m_\phi r} + \frac{y_\nu^2}{16\pi^2} \mathcal{V}(m_\phi r) \right]. \quad (3.12)$$

Here $V_t(r)$ is the full potential, with the subscript t indicating that it arises from the t -channel diagram. In the upper panel of Fig. 3, we present the full potential $V_t(r)$, together with its long- and short-range limits. In the shown example, we take $y_\nu = y_\chi = 1$ and define the length scale R as

$$R \equiv m_\phi^{-1} \quad (\text{for } t\text{-channel}). \quad (3.13)$$

It is clear that at short distances ($r \ll R$), the whole potential is dominated by the tree-level contribution, while in the long-range limit ($r \gg R$) it is dominated by the loop-level $1/r^5$ contribution since the tree-level Yukawa potential decreases exponentially with the distance.

3.2 The s -channel behavior

Next, let us consider that the effective vertex opens with an s -channel mediator—see the box diagram in Fig. 1. The Lagrangian we consider is given by

$$\mathcal{L}_{\text{int}} \supset y\bar{\chi}\nu\phi + \text{h.c.}, \quad (3.14)$$

where ϕ is a complex scalar field of mass m_ϕ . We note here that after integrating out ϕ and rearranging the fermionic fields via Fierz transformations, Eq. (3.14) gives rise to not only a contact interaction of the scalar form but also other contact interactions such as vector and tensor interactions. Since in this work we are interested in the r dependence rather than the spin dependence, the inclusion of these additional contact interactions is beyond the scope of this work.

With the interaction in Eq. (3.14) and the box diagram in Fig. 1, we write down the amplitude of $\chi\bar{\chi} \rightarrow \chi\bar{\chi}$ scattering:

$$i\mathcal{M} = -|y|^4 \int \frac{d^4 k}{(2\pi)^4} \bar{v}(p_2) \frac{i}{k} u(p_1) \bar{u}(p_3) \frac{i}{k - \not{p}_4} v(p_4) \frac{i}{(p_1 - k)^2 - m_\phi^2} \frac{i}{(p_2 + k)^2 - m_\phi^2}, \quad (3.15)$$

where p_1 (p_3) and p_2 (p_4) denote, respectively, the momenta of initial (final) momenta of χ and $\bar{\chi}$. In addition, the extra minus sign comes from the odd-number interchanges of anticommuting operators. Since the wave functions (u, v) only depend on the external momenta, they can be extracted out of the integral, leading to

$$i\mathcal{M} = -|y|^4 \bar{v}(p_2) \gamma_\mu u(p_1) \bar{u}(p_3) \gamma_\nu v(p_4) I^{\mu\nu}, \quad (3.16)$$

where

$$I^{\mu\nu} = \int \frac{d^4k}{(2\pi)^4} \frac{k^\mu (k-q)^\nu}{k^2 (k-q)^2 \left[(p_1 - k)^2 - m_\phi^2 \right] \left[(p_2 + k)^2 - m_\phi^2 \right]}. \quad (3.17)$$

Note that, as a common feature of box diagrams, the loop integral is UV finite.

After performing the loop integral in Eq. (3.17), we obtain terms proportional to $g^{\mu\nu}$, $q^\mu q^\nu$, $p_i^\mu p_j^\nu$, $p_i^\mu q^\nu$, $p_i^\nu q^\mu$, with $i, j = 1, 2$. It can be shown that by taking the leading order of the non-relativistic limit, only the $g^{\mu\nu}$ term contributes. For the $g^{\mu\nu}$ term, we take only the spin-independent⁴ part and obtain the following potential:

$$V_s(r) = -\frac{3|y|^4}{128\pi^3 r} \int_0^\infty dt e^{-\sqrt{t}r} \left[\frac{1}{2A} + \frac{B^2 - tA}{4AB\sqrt{t}A} \ln \left(\frac{B - \sqrt{t}A}{B + \sqrt{t}A} \right) \right], \quad (3.18)$$

where $A \equiv t - 4m_\chi^2$, $B \equiv t + 2\Delta^2$ and

$$\Delta \equiv \sqrt{m_\phi^2 - m_\chi^2}. \quad (3.19)$$

Here we have assumed $m_\phi > m_\chi$ otherwise χ would be unstable. Similar to Eq. (3.13), we also define a length scale:

$$R \equiv \Delta^{-1} \quad (\text{for } s\text{-channel}). \quad (3.20)$$

The potential can be expanded in different ways to obtain different limits as we will present below. One should note, however, that the potential is only valid in the range of $r \gg m_\chi^{-1}$ since the external fermions should keep non-relativistic. Therefore, we may encounter several possible hierarchies depending the comparison of R with m_χ^{-1} and r .

The simplest case is $R < m_\chi^{-1}$. In this case, we only need to consider one possible hierarchy: $R < m_\chi^{-1} \ll r$. And the result simply reduces to

$$V_s(r) = -\frac{3|y|^4 R^4}{128\pi^3 r^5} \quad (R < m_\chi^{-1} \ll r). \quad (3.21)$$

It implies that the $1/r^5$ behavior remains valid as r decreases until r approaches m_χ^{-1} .

If $m_\chi^{-1} < R$ (for better illustration, we consider $m_\chi^{-1} \ll R$, which is the case in Ref. [13]), then it becomes more complicated. As r decreases from sufficiently large values, the $1/r^5$ behavior becomes invalid when r approaches a point where $m_\chi^{-1}/R \sim R/r$ (i.e. $r \sim m_\chi R^2$). After passing this point, the $1/r^5$ behavior is altered to $1/r^4$. Further, when it passes R (which is smaller than $m_\chi R^2$), it changes to $1/r^2$ and remains in this form until the non-relativistic approximation becomes invalid. The short-, intermediate- and long-range limits of the potential are given as follows:

$$V_s(r) = -\frac{3|y|^4}{128\pi^3} \times \begin{cases} \frac{\pi}{4m_\chi r^2} & (m_\chi^{-1} \ll r \ll R) \\ \frac{\pi R^2}{4m_\chi r^4} & (R \ll r \ll m_\chi R^2) \\ \frac{R^4}{r^5} & (m_\chi R^2 \ll r) \end{cases}. \quad (3.22)$$

In the lower panel of Fig. 3, we present the full potential $V_s(r)$ given by Eq. (3.18), together with

⁴The contribution from spin-dependent terms to the neutrino forces can be averaged out in spin summation.

the three limits in Eq. (3.22). In the shown example, we set $y = 1$ and $m_\chi = 100/R$. Hence the valid ranges for the aforementioned short, intermediate- and long-range limits are $10^{-2} \ll r/R \ll 1$, $1 \ll r/R \ll 10^2$, and $10^2 \ll r/R$, respectively.

4 Summary

In this paper, we investigate the short-range behavior of the neutrino forces which arise from the exchange of a pair of neutrinos between two fermions. Although in the SM, the interaction between neutrinos and external fermions can be effectively described by a contact vertex which leads to a $1/r^5$ potential, this may be not the case in new physics scenarios (in particular, for DM interactions), where the contact interaction might be invalid before the non-relativistic approximation of external fermions fails. Thus it is necessary to study possible variations of the potential in such cases.

We consider two possible scenarios to open up the contact vertex by introducing a t -channel or an s -channel mediator. In the t -channel scenario, the potential induced by the neutrino loop is given in Eqs. (3.4)-(3.5). In the long-range limit, it decreases with $1/r^5$ as expected while in the short-range limit it evolves as $\ln(m_\phi r)/r$. Including the tree-level Yukawa contribution, the full potential in the t -channel scenario is given in Eq. (3.12) and its behavior is shown in the upper panel of Fig. 3. For $1/m_\chi \ll r \ll 1/m_\phi$, the full potential is dominated by the tree-level contribution which behaves as $1/r$, while for $r \gg 1/m_\phi$ it is dominated by the loop-level $1/r^5$ contribution since the tree-level Yukawa potential decreases exponentially.

In the s -channel scenario, the neutrino potential is induced by the box diagram, with the complete expression given in Eq. (3.18) and an example shown in the lower panel of Fig. 3. The potential exhibits different behaviors as the distance approaches different limits: for the long-range limit $r \gg m_\chi/(m_\phi^2 - m_\chi^2)$, it behaves as $1/r^5$ as expected; for the intermediated-range limit $1/\sqrt{m_\phi^2 - m_\chi^2} \ll r \ll m_\chi/(m_\phi^2 - m_\chi^2)$, it behaves as $1/r^4$; and for the short-range limit $1/m_\chi \ll r \ll 1/\sqrt{m_\phi^2 - m_\chi^2}$, it behaves as $1/r^2$.

We emphasize that although the analysis in the present paper is performed only on the scalar-type and non-chiral interactions for the purpose of illustration and simplicity, the generalizations to the cases of chiral interactions or interactions with other Lorentz structures are straightforward.

Our results might be of potential importance to the study of long-range force effects in particle physics and cosmology.

Acknowledgements

The authors would like to thank Rupert Coy, Jichen Pan, Michel Tytgat, Di Zhang, and Shun Zhou for helpful discussions.

A Renormalization of the ϕ propagator

The neutrino loop that contributes to the two-point function of ϕ in Sec. 3.1 is UV divergent. In order to obtain its physical contribution, we shall renormalize the ϕ field and its mass.⁵ Following the

⁵The renormalization of y_ν does not affect the calculation of the self-energy of ϕ , thus we can simply identify y_ν as the finite renormalized quantity in our calculation.

standard renormalization procedure, we denote the bare field strength and the mass by ϕ_0 and m_0 , and the physical ones by ϕ and m_ϕ , respectively. The renormalization is hence formulated as

$$\phi_0 = Z_\phi \phi \equiv (1 + \delta_\phi) \phi, \quad m_0^2 = Z_m m_\phi^2 \equiv (1 + \delta_m) m_\phi^2. \quad (\text{A.1})$$

The bare self-energy of the scalar under the dimensional regularization, to the order of $\mathcal{O}(y_\nu^2)$, is given by

$$i\Sigma_2^0(q^2) = -(iy_\nu)^2 \int \frac{d^4k}{(2\pi)^4} \text{Tr} \left(\frac{i}{k} \frac{i}{k+q} \right) = \frac{iy_\nu^2}{8\pi^2} q^2 \left[2 + \Delta_E + \ln \left(\frac{\mu^2}{-q^2} \right) \right], \quad (\text{A.2})$$

where the extra minus sign comes from the neutrino loop, μ is the renormalization scale, $\Delta_E \equiv 1/\epsilon - \gamma_E + \ln(4\pi)$ with $\epsilon \rightarrow 0_+$ and $\gamma_E \approx 0.577$ being the Euler–Mascheroni constant.

The renormalized self-energy is a combination of the bare one plus the counterterms arising from Eq. (A.1):

$$\Sigma_2(q^2) = \Sigma_2^0(q^2) + q^2 \delta_\phi - m_\phi^2 (\delta_\phi + \delta_m). \quad (\text{A.3})$$

The counterterms are determined by the on-shell renormalization conditions⁶:

$$\text{Re} \Sigma_2(q^2) \Big|_{q^2=m_\phi^2} = 0, \quad \frac{d}{dq^2} \text{Re} \Sigma_2(q^2) \Big|_{q^2=m_\phi^2} = 0. \quad (\text{A.4})$$

Substituting Eq. (A.3) into Eq. (A.4), we solve it with respect to δ_m and δ_ϕ :

$$\begin{aligned} \delta_m &= \frac{1}{m_\phi^2} \text{Re} \Sigma_2^0(q^2) \Big|_{q^2=m_\phi^2} = \frac{y_\nu^2}{8\pi^2} \left[2 + \Delta_E + \ln \left(\frac{\mu^2}{m_\phi^2} \right) \right], \\ \delta_\phi &= -\frac{d}{dq^2} \text{Re} \Sigma_2^0(q^2) \Big|_{q^2=m_\phi^2} = -\frac{y_\nu^2}{8\pi^2} \left[1 + \Delta_E + \ln \left(\frac{\mu^2}{m_\phi^2} \right) \right]. \end{aligned} \quad (\text{A.5})$$

Then the renormalized self-energy is determined by substituting Eq. (A.5) back into Eq. (A.3):

$$\Sigma_2(q^2) = \frac{y_\nu^2}{8\pi^2} \left[(q^2 - m_\phi^2) + q^2 \ln \left(\frac{m_\phi^2}{-q^2} \right) \right]. \quad (\text{A.6})$$

Note that the self-energy of ϕ in Eq. (A.6) has an imaginary part when it goes on-shell, $q^2 = m_\phi^2$. This corresponds to the instability of ϕ : it can decay into a pair of neutrinos with the decay rate $\Gamma_\phi = y_\nu^2 m_\phi / (8\pi)$. However, for the non-relativistic t -channel scattering process we consider throughout this paper, the momentum transfer q is always spacelike, namely $q^2 < 0$, thus the amplitude is always real. Finally, the renormalized amplitude is given by

$$\begin{aligned} i\mathcal{A}(q^2) &= (iy_\chi)^2 \frac{i}{q^2 - m_\phi^2} i\Sigma_2(q^2) \frac{i}{q^2 - m_\phi^2} \\ &= \frac{iy_\chi^2 y_\nu^2}{8\pi^2 (q^2 - m_\phi^2)^2} \left[(q^2 - m_\phi^2) - q^2 \ln \left(\frac{-q^2}{m_\phi^2} \right) \right], \end{aligned} \quad (\text{A.7})$$

⁶Note that for unstable particles, since their on-shell self-energy contains imaginary parts, the on-shell renormalization conditions fix the real parts [35, 36].

where the normalized factor $1/(4m_\chi^2)$ has been cancelled by the non-relativistic wave functions of external fermions. The amplitude in Eq. (A.7) is finite.

B Branch cuts and singularities of the amplitude

In this appendix, we present in detail the calculations of the Fourier integrals used in this work.

For neutrino forces from contact interactions, we encounter the following integral:

$$\begin{aligned}
I_c &\equiv - \int \frac{d^3 \vec{q}}{(2\pi)^3} e^{i\vec{q}\cdot\vec{r}-|\vec{q}\cdot\vec{r}|0_+} \left[C - q^2 \ln\left(-\frac{q^2}{\mu^2}\right) \right] \\
&= \frac{i}{4\pi^2 r} \int_{-\infty}^{\infty} d\rho e^{i\rho r} \rho \left[C + \rho^2 \ln\left(\frac{\rho^2}{\mu^2}\right) \right] \\
&= \frac{i}{4\pi^2 r} \int_0^{\infty} i d\rho_i e^{-\rho_i r} i^3 \rho_i^3 \left[\ln\left(\frac{-\rho_i^2 + i0_+}{\mu^2}\right) - \ln\left(\frac{-\rho_i^2 - i0_+}{\mu^2}\right) \right] \\
&= \frac{i}{4\pi^2 r} \int_0^{\infty} d\rho_i e^{-\rho_i r} \rho_i^3 \times 2\pi i \\
&= -\frac{3}{\pi r^5}. \tag{B.1}
\end{aligned}$$

Here C is some quantity that does not have singularities or branch cuts on the imaginary axis of ρ , $q^2 = q_\mu q^\mu = -|\vec{q}|^2$, $\rho \equiv |\vec{q}|$, ρ_i is the imaginary part of ρ (on the imaginary axis, $\rho = i\rho_i$), and 0_+ denotes a positive infinitesimal number. The logarithmic part contains a branch cut on the imaginary axis. Hence in the third step we push the contour upward so that it becomes an integral along the imaginary axis.

To study neutrino forces with the t -channel behavior, we need to compute the following integral:

$$\begin{aligned}
I_t &\equiv - \int \frac{d^3 \vec{q}}{(2\pi)^3} \frac{e^{i\vec{q}\cdot\vec{r}-|\vec{q}\cdot\vec{r}|0_+}}{(q^2 - m^2)^2} \left[q^2 - m^2 - q^2 \ln\left(-\frac{q^2}{m^2}\right) \right] \\
&= \frac{i}{4\pi^2 r} \int_{-\infty}^{\infty} d\rho e^{i\rho r} \rho \frac{\rho^2 \ln\left(\frac{\rho^2}{m^2}\right) - \rho^2 - m^2}{(\rho^2 + m^2)^2}. \tag{B.2}
\end{aligned}$$

The integrand contains both singularities (at $\rho = \pm im$) and a branch cut on the imaginary axis, as shown in Fig. 4. To compute the integral, we slightly pull the singularities off the imaginary axis so that the integral can be converted to an integral around one of the singularities and an integral along the branch cut. Specifically, we replace the integrand with the following function:

$$f(\rho, \epsilon) \equiv e^{i\rho r} \rho \frac{\rho^2 \ln\left(\frac{\rho^2}{m^2}\right) - \rho^2 - m^2}{(\rho^2 + m^2 - i\epsilon)^2}, \quad (\epsilon \rightarrow 0_+). \tag{B.3}$$

The residue of f at the $\rho = i\sqrt{m^2 - i\epsilon}$ singularity contributes the following part to the integral:⁷

$$2\pi i \lim_{\epsilon \rightarrow 0_+} \text{Res} \left[f(\rho = i\sqrt{m^2 - i\epsilon}, \epsilon) \right] = \frac{\pi^2}{2} e^{-mr} (mr - 2). \tag{B.4}$$

⁷If we had pulled the singularities to the opposite direction by replacing $i\epsilon$ with $-i\epsilon$ in Eq. (B.3), the residue in Eq. (B.4) would differ by a minus sign. However, as one can check, the contribution of the branch cut in this case would also change while the total contribution remains the same.

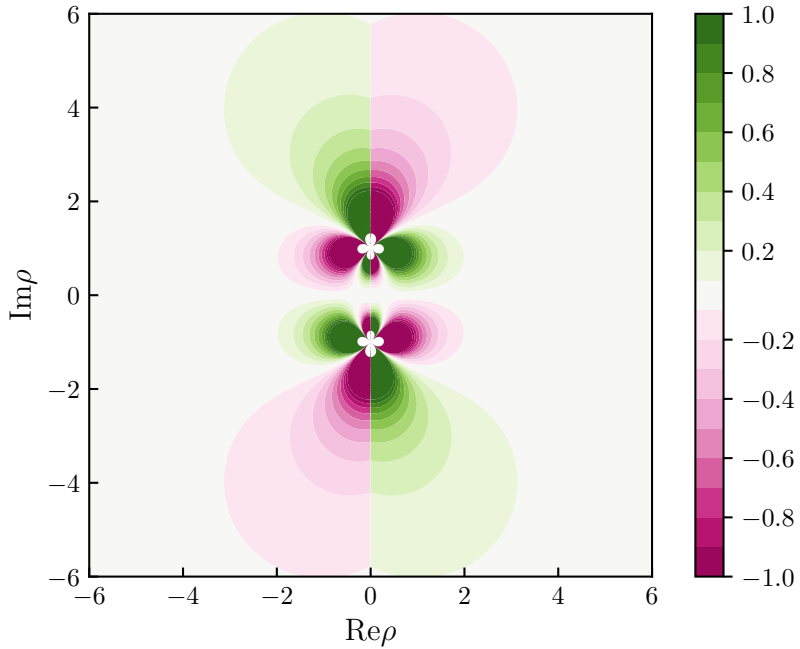


Figure 4. Contours of $\text{Im} \left\{ (\rho^2 + m^2)^{-2} [\rho^2 \ln(\rho^2/m^2) - \rho^2 - m^2] \right\}$, to show branch cuts (on the imaginary axis) and singularities (at $\rho = \pm im$ with $m = 1$) of the integrand in Eq. (B.2).

The branch cut along the positive part of the imaginary axis contributes to the integral as follows:

$$\begin{aligned} \int_0^\infty i d\rho_i \lim_{\rho_r \rightarrow 0^+} [f(i\rho_i + \rho_r, \epsilon) - f(i\rho_i - \rho_r, \epsilon)] &= 2\pi i \int_0^\infty d\rho_i \frac{\rho_i^3 e^{-\rho_i r}}{(\rho_i^2 - m^2 + i\epsilon)^2} \\ &= -\frac{\pi^2}{2} e^{-mr} (mr - 2) - \frac{i\pi}{2} mr \mathcal{V}(mr), \end{aligned} \quad (\text{B.5})$$

where the \mathcal{V} function was defined in Eq. (3.5).

Combining the results in Eqs. (B.4) and (B.5), we obtain

$$I_t = \frac{m}{8\pi} \mathcal{V}(mr). \quad (\text{B.6})$$

For the s -channel case, the corresponding Fourier integral cannot be expressed in terms of known special functions. However, we can follow similar steps to convert it to an integral along the imaginary axis. This leads to the integral in Eq. (3.18).

References

- [1] H. Bethe and R. A. Bacher, Rev. Mod. Phys. 8, 201 (1936); D. Iwanenko and A. Sokolow, Z. Physik 102, 119 (1936); G. Gamow and E. Teller, Phys. Rev. 51, 289 (1937).
- [2] G. Feinberg and J. Sucher, *Long-Range Forces from Neutrino-Pair Exchange*, Phys. Rev. **166** (1968) 1638–1644.

- [3] G. Feinberg, J. Sucher, and C. K. Au, *The dispersion theory of dispersion forces*, *Phys. Rept.* **180** (1989) 83.
- [4] S. D. H. Hsu and P. Sikivie, *Long range forces from two neutrino exchange revisited*, *Phys. Rev. D* **49** (1994) 4951–4953, [[hep-ph/9211301](#)].
- [5] G. Feinberg and J. Sucher, *Long-Range Electromagnetic Forces on Neutral Particles*, *Phys. Rev.* **139** (1965) B1619.
- [6] A. Segarra, *Neutrino-pair exchange long-range force between aggregate matter*, Master's thesis, Valencia U., 7, 2015.
- [7] Q. Le Thien and D. E. Krause, *Spin-independent two-neutrino exchange potential with mixing and cp-violation*, *Phys. Rev. D* **99** (2019), no. 11 116006, [[1901.05345](#)].
- [8] Z.-z. Xing, *Flavor structures of charged fermions and massive neutrinos*, *Phys. Rept.* **854** (2020) 1–147, [[1909.09610](#)].
- [9] J. A. Grifols, E. Masso, and R. Toldra, *Majorana neutrinos and long range forces*, *Phys. Lett. B* **389** (1996) 563–565, [[hep-ph/9606377](#)].
- [10] A. Segarra and J. Bernabéu, *Absolute neutrino mass and the dirac/majorana distinction from the weak interaction of aggregate matter*, *Phys. Rev. D* **101** (2020), no. 9 093004, [[2001.05900](#)].
- [11] A. Costantino and S. Fichet, *The neutrino casimir force*, *JHEP* **09** (2020) 122, [[2003.11032](#)].
- [12] M. Lusignoli and S. Petrarca, *Remarks on the forces generated by two-neutrino exchange*, *Eur. Phys. J. C* **71** (2011) 1568, [[1010.3872](#)].
- [13] N. Orlofsky and Y. Zhang, *Neutrino as the dark force*, *Phys. Rev. D* **104** (2021), no. 7 075010, [[2106.08339](#)].
- [14] S. Fichet, *Quantum forces from dark matter and where to find them*, *Phys. Rev. Lett.* **120** (2018), no. 13 131801, [[1705.10331](#)].
- [15] P. Brax, S. Fichet, and G. Pignol, *Bounding quantum dark forces*, *Phys. Rev. D* **97** (2018), no. 11 115034, [[1710.00850](#)].
- [16] A. Costantino, S. Fichet, and P. Tanedo, *Exotic spin-dependent forces from a hidden sector*, *JHEP* **03** (2020) 148, [[1910.02972](#)].
- [17] H. Banks and M. Mccullough, *Charting the fifth force landscape*, *Phys. Rev. D* **103** (2021), no. 7 075018, [[2009.12399](#)].
- [18] G. Feinberg and J. Sucher, *The two photon exchange force between charged systems. 1. spinless particles*, *Phys. Rev. D* **38** (1988) 3763. [Erratum: *Phys. Rev. D* 44, 3997 (1991)].
- [19] G. Feinberg and J. Sucher, *Spin dependent two photon exchange forces: Spin0 particle and a charged spin 1/2 particle*, *Phys. Rev. D* **45** (1992) 2493–2517.
- [20] J. A. Grifols and S. Tortosa, *Residual long range pseudoscalar forces between unpolarized macroscopic bodies*, *Phys. Lett. B* **328** (1994) 98–102, [[hep-ph/9404249](#)].
- [21] F. Ferrer and J. A. Grifols, *Long range forces from pseudoscalar exchange*, *Phys. Rev. D* **58** (1998) 096006, [[hep-ph/9805477](#)].
- [22] J. B. Hartle, *Long-range weak forces and cosmology*, *Phys. Rev. D* **1** (1970) 394–397.
- [23] C. J. Horowitz and J. T. Pantaleone, *Long range forces from the cosmological neutrinos background*, *Phys. Lett. B* **319** (1993) 186–190, [[hep-ph/9306222](#)].

- [24] F. Ferrer, J. A. Grifols, and M. Nowakowski, *Long range forces induced by neutrinos at finite temperature*, *Phys. Lett. B* **446** (1999) 111–116, [[hep-ph/9806438](#)].
- [25] E. Fischbach, *Long range forces and neutrino mass*, *Annals Phys.* **247** (1996) 213–291, [[hep-ph/9603396](#)].
- [26] A. Y. Smirnov and F. Vissani, *Long range neutrino forces and the lower bound on neutrino mass*, [hep-ph/9604443](#).
- [27] A. Abada, M. B. Gavela, and O. Pene, *To rescue a star*, *Phys. Lett. B* **387** (1996) 315–319, [[hep-ph/9605423](#)].
- [28] M. Kachelriess, *Neutrino selfenergy and pair creation in neutron stars*, *Phys. Lett. B* **426** (1998) 89–94, [[hep-ph/9712363](#)].
- [29] K. Kiers and M. H. G. Tytgat, *Neutrino ground state in a dense star*, *Phys. Rev. D* **57** (1998) 5970–5981, [[hep-ph/9712463](#)].
- [30] A. Abada, O. Pene, and J. Rodriguez-Quintero, *Finite size effects on multibody neutrino exchange*, *Phys. Rev. D* **58** (1998) 073001, [[hep-ph/9802393](#)].
- [31] J. Arafune and Y. Mimura, *Finiteness of multibody neutrino exchange potential energy in neutron stars*, *Prog. Theor. Phys.* **100** (1998) 1083–1088, [[hep-ph/9805395](#)].
- [32] Y. V. Stadnik, *Probing long-range neutrino-mediated forces with atomic and nuclear spectroscopy*, *Phys. Rev. Lett.* **120** (2018), no. 22 223202, [[1711.03700](#)].
- [33] M. Ghosh, Y. Grossman, and W. Tangarife, *Probing the two-neutrino exchange force using atomic parity violation*, *Phys. Rev. D* **101** (2020), no. 11 116006, [[1912.09444](#)].
- [34] A. Y. Smirnov and X.-J. Xu, *Wolfenstein potentials for neutrinos induced by ultra-light mediators*, *JHEP* **12** (2019) 046, [[1909.07505](#)].
- [35] K. I. Aoki, Z. Hioki, M. Konuma, R. Kawabe, and T. Muta, *Electroweak theory. framework of on-shell renormalization and study of higher order effects*, *Prog. Theor. Phys. Suppl.* **73** (1982) 1–225.
- [36] M. Bohm, H. Spiesberger, and W. Hollik, *On the one loop renormalization of the electroweak standard model and its application to leptonic processes*, *Fortsch. Phys.* **34** (1986) 687–751.